Xenobiotica, August 2006; 36(8): 724–737

Kinetics of paraquat in the isolated rat lung: Influence of sodium depletion

R. J. DINIS-OLIVEIRA[1,2], M. J. DE JESÚS VALLE[2], M. L. BASTOS[1], F. CARVALHO[1], & A. SÁNCHEZ NAVARRO[2]

[1]*Faculty of Pharmacy, Department of Toxicology, University of Porto, REQUIMTE, Porto, Portugal and* [2]*Department of Pharmacy and Pharmaceutical Technology, Faculty of Pharmacy, University of Salamanca, Salamanca, Spain*

(Received 20 December 2005)

Abstract

Paraquat accumulates in the lung through a characteristic polyamine uptake system. It has been previously shown that paraquat uptake can be significantly prevented if extracellular sodium (Na^+) is reduced, although the available data correspond to experiments performed using tissue slices or incubated cells. This type of *in vitro* study fails to give information on the actual behaviour occurring *in vivo* since the anatomy and physiology of the studied tissue is disrupted. Accordingly, the aim of the present study was to explore the usefulness of the isolated rat lung model when applied to characterize the kinetic behaviour of paraquat in this tissue after bolus injection under standard experimental conditions as well as to evaluate the influence of iso-osmotic replacement of Na^+ by lithium (Li^+) in the perfusion medium. The obtained results show that the present isolated rat lung model is useful for the analysis of paraquat toxicokinetics, which is reported herein for the first time. It was also observed that Na^+ depletion in the perfusion medium leads to a decreased uptake of paraquat in the isolated rat lung, although it seems that this condition does not contribute to improve the elimination of paraquat once the herbicide reaches the extravascular structures of the tissue, since the paraquat tissue wash-out phase is similar under both experimental conditions assayed.

Keywords: *Isolated rat lung, paraquat, toxicokinetics, sodium, lithium*

Introduction

Since its introduction in agriculture in 1962 (Onyeama and Oehme 1984), the widespread, non-selective contact herbicide paraquat, used as a desiccant and defoliant in a variety

Correspondence: A. Sánchez Navarro, Faculty of Pharmacy, Department of Pharmacy and Pharmaceutical Technology, University of Salamanca, Avda. Campo Charro s/n. 37007, Salamanca, Spain. Tel: 34-923-294536. Fax: 34-923-294515. E-mail: asn@usal.es

ISSN 0049-8254 print/ISSN 1366-5928 online
DOI: 10.1080/00498250600790331

of crops, has caused thousands of deaths from both accidental and voluntary ingestion, as well as from dermal exposure. It may be considered as one of the most toxic poisons frequently used for suicide attempts. Nevertheless, it is readily available without restriction in several countries where it is registered. Depending on the ingested dose, different clinical patterns and outcomes have been observed in animals and humans. A large oral dose of paraquat (>30 mg kg^{-1} in humans) rapidly leads to death from multi-organ failure, with lung damage consisting of disruption of the alveolar epithelial cells, haemorrhage, oedema, and infiltration of inflammatory cells into the interstitial and alveolar spaces. Smaller doses of paraquat (16 mg kg^{-1}) may also lead to death, but this occurs after several days as a result of a progressive lung fibrosis, by proliferation of fibroblasts and excessive collagen deposition showing that the main target organ for paraquat toxicity is the lung (Onyeama and Oehme 1984).

The direct cellular toxicity of paraquat is essentially due to its redox cycling (Figure 1): paraquat is reduced enzymatically, mainly by β-nicotinamide adenine dinucleotide phosphate (NADPH)-cytochrome P450 reductase (Clejan and Cederbaum 1989) and

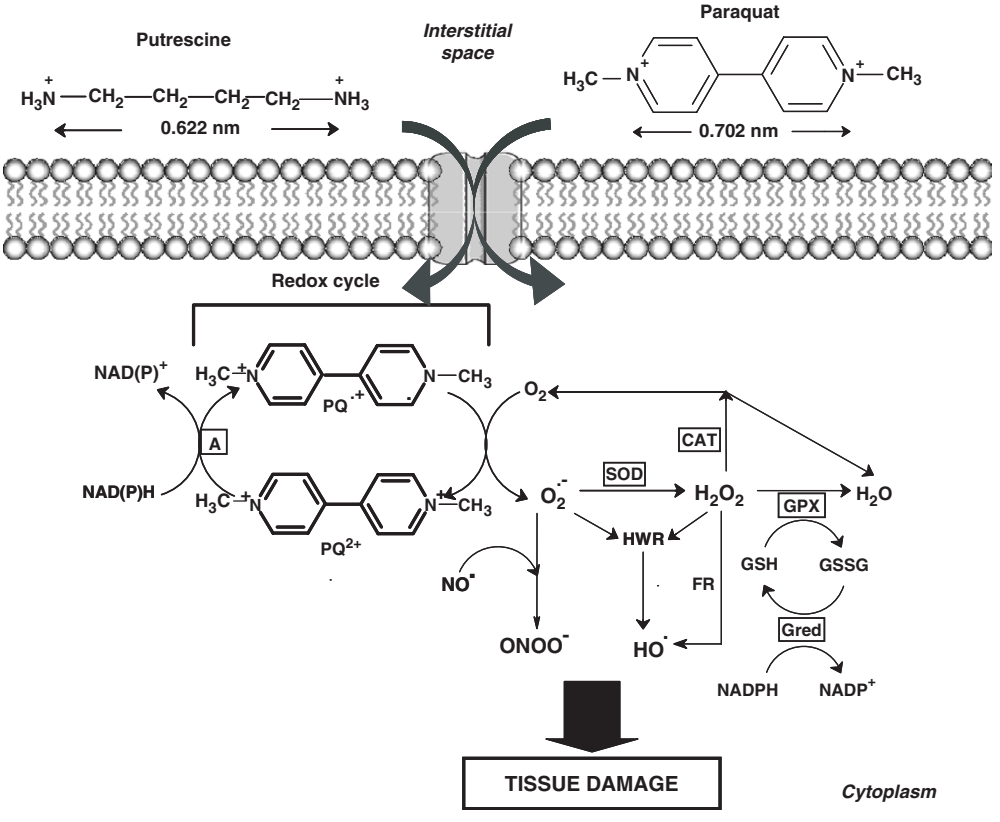

Figure 1. Schematic representation of the mechanism of paraquat toxicity. (A) Cellular diaphorases; SOD, superoxide dismutase or spontaneously; CAT, catalase; GPX, glutathione peroxidase; Gred, glutathione reductase; PQ^{2+}, paraquat; PQ^{+}, paraquat cation radical; FR, Fenton reaction; HWR, Haber–Weiss reaction.

NADH:ubiquinone oxidoreductase (complex I) (Fukushima et al. 1993; Yamada and Fukushima 1993) to form a paraquat monocation-free radical. The paraquat monocation-free radical is then rapidly reoxidized in the presence of oxygen, thus resulting in the generation of the superoxide radical ($O_2^{\bullet -}$) (Bus et al. 1974; Dicker and Cederbaum 1991). This then sets in the well-known cascade leading to generation of the hydroxyl radical and consequent deleterious effects. Indeed, hydroxyl radicals (Bus et al. 1975; Youngman and Elstner 1981) have been implicated in the initiation of membrane damage by lipid peroxidation during exposure to paraquat *in vitro* (Bus et al. 1975) as well as *in vivo* (Burk et al. 1980; Dicker and Cederbaum 1991) by attack on polyunsaturated lipids, the depolymerization of hyaluronic acid, the inactivation of proteins, and damage of DNA. Besides, researchers have recently suggested the hypothesis of cytotoxicity via mitochondrial dysfunction caused by paraquat (Blaszczynski et al. 1985; Hirai et al. 1985; Thakar and Hassan 1988; Tomita 1991; Fukushima et al. 1994; Tawara et al. 1996). The $O_2^{\bullet -}$ resulting from the paraquat redox-cycle may also react with nitric oxide ($NO^{\bullet}$) produced by nitric oxide synthase (NOS) leading to the formation of the toxic reactive species peroxynitrite anion ($ONOO^-$) (LaVoie and Hastings 1999), thus further contributing to paraquat damage.

Rose et al. (1974) demonstrated that the accumulation of radioactively labelled paraquat in rat lung slices was energy-dependent and obeyed saturation kinetics. Other studies led to the conclusion that paraquat accumulated in the lung through a system for which the polyamines are the natural substrates and that, in comparison with other organs, the lungs, and more specifically the alveolar epithelial cells, are endowed with a particularly active uptake system (Smith 1982; Rannels et al. 1985, 1989; Nemery et al. 1987; Dinsdale et al. 1991). An important aim of earlier studies concerning pulmonary polyamine uptake was to discover the structural requirements for substrates of the transport system in order to find possible antagonists capable of preventing paraquat from entering its target cells. Ross and Krieger (1981) established that to act as a substrate for the pulmonary polyamine uptake system, a molecule must possess the following characteristics: (1) two or more positively charged nitrogen atoms, (2) maximum positivity of charge surrounding these nitrogens, (3) a non-polar group between these charges, and (4) a minimum of steric hindrance. Gordonsmith et al. (1983) have demonstrated that the optimum distance between the nitrogen centres is four methylene groups (6.6 Å), although a spacing between four and seven methylene groups is tolerated. These data explain how polyamines and paraquat (with $\approx$7.0 Å between two positively charged nitrogens) can share a common uptake system, but also why paraquat (with its steric hindrance of the nitrogens by the pyridine rings) is a less successful substrate. Although paraquat proved to be a rather 'poor' substrate for the polyamine uptake system, it is undoubtedly accumulated into the lung through this transport pathway.

In a study performed in mice neuroblastoma cells (Rinehart and Chen 1984), the possibility of sodium (Na^+) requirement for putrescine uptake was examined by iso-osmotic replacement of Na^+ by choline or lithium (Li^+) in the incubation medium. The putrescine uptake decreased with decreasing extracellular Na^+ concentration, suggesting a strong Na^+ dependency of the polyamine uptake system. Na^+ replacement by Li^+ was also demonstrated to inhibit significantly putrescine uptake by rat isolated enterocytes (Kumagai and Johnson 1988). In bovine arterial smooth muscle cells, Janne et al. (1978) and Aziz et al. (1994) demonstrated some Na^+ dependence for polyamine uptake. Rannels et al. (1989)

found that in type II pneumocytes the uptake of putrescine and spermidine was dependent on Na^+, whereas spermine uptake was not dependent on extracellular Na^+, indicating that polyamine uptake may take place via different transporters systems. Like putrescine, uptake of the herbicide paraquat was extensively inhibited as extracellular Na^+ was reduced.

The various studies mentioned above suggest that paraquat, like some polyamines, shows cell uptake depending on Na^+ levels, particularly in type II pneumocytes. Nevertheless, the available data correspond to experiments performed using tissue slices or incubated cells. This latter type of *in vitro* studies provide information about the intrinsic affinity of a compound for the incubated structure but fails to give information on the actual behaviour occurring *in vivo* since the anatomy and physiology of the studied tissue is disrupted.

The isolated tissue and artificial perfusion techniques facilitate the performance of studies aimed at characterizing the intrinsic behaviour of a compound in a particular tissue with no interference of the rest of the body while maintaining its anatomical integrity and physiological properties. Accordingly, the aim of the present study was to explore the usefulness of the isolated rat lung model when applied to the characterization of the kinetic behaviour of paraquat in this tissue under standard experimental conditions as well as to evaluate the influence of iso-osmotic replacement of Na^+ by Li^+ in the perfusion medium on the kinetics of this xenobiotic in pulmonary tissue.

Materials and methods

Reagents

Paraquat dichloride (purchased as methylviologen, 98% chemical purity) and fraction V bovine serum albumin were obtained from Sigma-Aldrich (USA). Other reagents such as NaCl, KCl, $CaCl_2$, KH_2PO_4, $MgSO_4 \cdot 7H_2O$, $NaHCO_3$, NaOH, glucose, sodium dithionite, sulfosalicylic acid and lithium chloride were obtained from Panreac (Spain). Heparin 5000 UI ml^{-1} and sodium thiopental were obtained from B. Braun (Spain).

Perfusion medium composition

The perfusion medium was a modified Krebs–Henseleit bicarbonate buffer, pH 7.4, equilibrated with a carbogen mixture (95% O_2, 5% CO_2) and containing NaCl (119 mM), KCl (4.7 mM), $CaCl_2$ (3.6 mM), KH_2PO4 (1.18 mM), $MgSO_4 \cdot 7H_2O$ (1.18 mM), $NaHCO_3$ (25 mM), glucose (5 mM) and fraction V bovine serum albumin (3%; wt/vol.).

Sodium replacement

The NaCl (119 mM) present in the Krebs–Henseleit medium was replaced by an equal molar concentration of LiCl.

Animals

The study was performed using 20 adult male rats (SLC: Wistar strain) with a mean body weight of 263.2 ± 13.0 g. The animals were divided into two experimental groups. One group ($n = 10$) was assigned as control group whereas another ($n = 10$) was assigned as the Li^+ perfusion group. The animals were maintained with water and food (standard laboratory chow) (Agway RMH-3000 chow) *ad libitum* until the moment of anaesthesia, which was induced with sodium thiopental ($60\,mg\,kg^{-1}$, intraperitoneally). Housing (in Plexi-glass cages) and the experimental treatment of animals were in accordance with National Institutes of Health guidelines. The experiments complied with the current laws of Spain and Portugal.

Isolated lung model: Surgical procedure

The method used to isolate lungs and to keep them artificially perfused and mechanically ventilated has been described previously (Martinez et al. 2005). Briefly, it consists of the following steps:

- Tracheotomy and tracheal cannulation of the animals placed in the *decubito supino* position on an electric blanket heated at 37°C, followed by the immediate connection of the cannula to a mechanical ventilation system and subsequent injection of sodium heparin through the intraperitoneal route. The ventilation system works under positive pressure and provides warmed and moistened air to the lungs.
- Opening of the thorax by two lateral transversal and one central longitudinal incision to expose the thoracic viscera.
- Localization of the pulmonary and aortic arteries to place a loose ligature around both vessels in a position very close to the heart.
- Incision of the left ventricle, insertion of a previously heparinized outflow cannula and fixation of the cannula by clamping.
- Incision of the right ventricle, insertion of a heparinized inflow cannula and tying the ligature previously placed to fix the cannula just before the bifurcation of the pulmonary artery. The inflow cannula was connected to the mechanical pump before its insertion to initiate artificial perfusion of the lungs at the same moment as the blood supply to the tissue was interrupted. After a stabilization period of 5 min to wash out residual blood elements from the pulmonary circulation, paraquat was injected and a sample collection of efferent fluid was started.

Experimental monitoring

- Visualization of the preparation at the start of the perfusion to check that the whole lung was properly perfused. The presence of local areas with a slow washout of blood indicated deficiencies in the procedure and was a criterion for the non-viability of the experimental model.
- Visualization of the preparation throughout the experimental procedure in order to verify that no tissue oedema was present. The development of translucent areas as the

experiments progressed indicated deficiencies in the procedure and was a criterion for the non-viability of the experimental model.
- Continuous measurement and recording of the flow rate and hydrostatic pressure at arterial level, using a probe and pressure transducer connected to the inflow cannula and to the corresponding data acquisition software. A flow rate and a hydrostatic pressure out of the interval 5 ± 0.5 ml and 13 ± 2 mm Hg were considered as criteria of non-viability of the experimental model.

Experimental equipment

The main elements of the system and the experimental conditions selected were the following:

- Rodent ventilator (7025 Ugo Basile): this element was pre-set to supply a tidal volume of 2 ml at a respiratory frequency of 60 rpm with room air previously conditioned at 37°C and saturated humidity. Conditioning of the air prior to its supply to the animals was carried out by connecting the ventilator to a double-jacketed chamber into which atmospheric air was bubbled through water at 37°C. The ventilator took the air from this chamber instead of supplying non-conditioned atmospheric air.
- Perfusion pump (Minipuls® 3 Gilson): provided a non-pulsatile flow rate of 5 ml min^{-1} of the perfusion medium Krebs–Henseleit bicarbonate (pH 7.4) with glucose (0.9 g l^{-1}) and bovine albumin (fraction V, 30 g l^{-1}) in the standard and Na^{+}-replaced medium conditions.
- Oxygenating bubbler: permits the perfusion media to be gassed effectively, with a mixture of 95% of O_2 and 5% of CO_2, 10 min prior to starting the perfusion and throughout the experiments.
- Bubble trap: prevents the presence of air bubbles in the medium supplied to the isolated lung.
- Thermostatted bath: maintains water at 37°C circulating through the double-jacketed elements.
- Fraction collector (Gilson FC 203B Fraction Collector): this was connected to the outflow cannula and programmed to collect efferent fluid at the following sampling times after the dose injection: 3-s intervals for the first 1 min, and 6-s intervals over the next 1 min. Subsequently, sampling time intervals were 10 s for the next 2 min; 20 s for the next 2 min; 30 s for the next 2 min and 60 s for the next 12 min (a total sampling time 20 min and total samples = 64).
- Flow and pressure-control device: a probe (Transonic Systems, Inc. T106) was connected to the inflow cannula to measure the flow rate and corresponding pressure transducer (Transpac® IV, Abbott Critical Care) was fitted to determine the hydrostatic pressure at the arterial level.
- Data acquisition software: the Windaq (DATAQ Instruments WINDAQ, Version 1.91) program was used to record and file all the data concerning flow rate and pressure throughout the experiments.

Drug injection

Five minutes after the start of the artificial perfusion (stabilization period), 1000 μg of paraquat dissolved in 250 μl of perfusion medium were introduced through the Y-device of the inflow cannula as a bolus injection.

All the experimental conditions were the same in both groups, except for Na^+ levels in the perfusion medium, which was replaced in one of the groups by Li^+ at an iso-osmotic level.

Sample pretreatment

After 20 min of perfusion and sampling collection, all major cartilaginous airways were dissected free and the wet weight of the remaining lung tissue was determined. The lungs were then processed for the measurement of the remaining paraquat. The lung tissue was homogenized (Pro 250 Homogenizer) in 50 mM phosphate buffer/0.1% Triton X-100 (pH 7.4). The homogenate was kept on ice and then centrifuged at 13 000*g*, 4°C for 20 min. Aliquots of the resulting supernatants were treated with sulfosalicylic acid (5% in final volume) and centrifuged (13 000*g*, 4°C for 5 min). Aliquots of the outflow samples were also treated with sulfosalicylic acid (5% in final volume) to precipitate the proteins and centrifuged (13 000*g*, 4°C for 5 min). After deproteinization, the supernatants were alkalinized with 10 N NaOH (pH > 9) and then gently mixed with the reductant (sodium dithionite) to give a blue colour characteristic of the paraquat radical. In two animals of each group the perfusion was prolonged until 30 min in order to evaluate the effect of this substitution in the viability criteria referred to above (hydrostatic pressure increase and appearance of translucent areas).

Paraquat analysis

Paraquat quantitation in outflow perfusate and lung homogenates was carried out using a rapid, simple method based on second-derivative spectrophotometry (Fell et al. 1981; Fuke et al. 1992; Kuo et al. 2001) using a Shimadzu model UV/VIS 160 double-beam with a built-in microcomputer and a quartz cell with an optical path length of 1.0 cm. No interference was observed in the zero-order and second-derivative spectrum of the blank. The data of a zero-order spectrum obtained by scanning from 500 to 380 nm with a 0.5-nm bandwidth were stored in the machine and then differentiated with 4 nm of differential wavelength to give a second derivative spectrum. A qualitative and quantitative analysis of reduced paraquat was made at the amplitude peaks of 396–403 nm of the second-derivative spectrum. The calibration curve in the 0.2–8.0 $\mu g\,ml^{-1}$ range obeys Beer's law. The samples were diluted in order to fall into the reference range of the standard curve.

Using these experimental conditions, the intra- and inter-day coefficients of variation showed values lower than 5% and the detection limit of the method was 100 $ng\,ml^{-1}$.

Results for the lungs were expressed in $\mu mol\,PQ\,mg^{-1}$ protein. Lung protein quantification was performed according to the method of Lowry et al. (1951), using bovine serum albumin as standard.

Toxicokinetic analysis

Paraquat concentration curves in the lung efferent fluid were analysed by the statistical moment theory (Yamaoka et al. 1978). According to this theory, the area under the curve (AUC), mean transit time (MTT) and variance of transit time (VTT) may be estimated in the isolated lung from the stochastic analysis of the outflow concentration curve (C_t)

using the following equations:

$$\mathrm{AUC}_0^{\infty} = \int_0^{\infty} C(t)\mathrm{d}t \tag{1}$$

$$\mathrm{MTT} = \frac{\int_0^{\infty} t \cdot C(t)\mathrm{d}t}{\int_0^{\infty} C(t)\mathrm{d}t} \tag{2}$$

$$\mathrm{VTT} = \frac{\int_0^{\infty} (t - \mathrm{MTT})^2 \cdot C(t)\mathrm{d}t}{\int_0^{\infty} C(t)\mathrm{d}t} \tag{3}$$

Since the experimental system used here included tubing besides the isolated tissue, it was necessary to correct for the influence of these devices on the MTT estimated from the above equation. Additional experiments performed under the same experimental conditions as described above, but in absence of the tissue were carried out to quantify the mean transit time of the drug in the devices ($\mathrm{MTT_d}$), in order to estimate the actual mean transit time of the drug in the tissue ($\mathrm{MTT_a}$) by applying the following correction:

$$\mathrm{MTT_a} = \mathrm{MTT} - \mathrm{MTT_d} \tag{4}$$

Assuming the experimental preparation as an stationary system, the volume of distribution of the drug in the lung (V_d) was calculated from the mean transit time of paraquat in the tissue ($\mathrm{MTT_a}$) and the perfusion flow rate ($Q = 5\,\mathrm{ml\,min^{-1}}$), as follows (Weiss 1995):

$$V_d = \mathrm{MTT_a} \cdot Q \tag{5}$$

The distribution coefficient (V_d/L_w) was also calculated, L_w being the weight of the isolated lung. Finally, the washout rate constant (K_w) was estimated from the slope value of the terminal phase of the outflow curve.

Statistical analysis

Results are given as the mean ± standard deviation (SD). Statistical comparison of parameters obtained for paraquat in both groups was performed by a Student's *t*-test for non-paired samples using the STATGRAPHICS Plus 4.0 program. The level of significance was set at $p < 0.05$.

Results

Figure 2 shows the mean concentration curves of paraquat in the efferent fluid for control and Na^+-depleted medium groups with the corresponding standard deviations. Very similar concentration profiles in the outflow fluid are observed, although some interesting differences must be highlighted. In fact, a peak value is rapidly achieved in both groups. Nevertheless, the mean value of the peak concentration reaches a higher value in the Li^+ group (679.62 ± 43.04 vs. $491.59 \pm 29.00\,\mu\mathrm{g\,ml^{-1}}$; $p < 0.001$). This result is supported and confirmed by the results

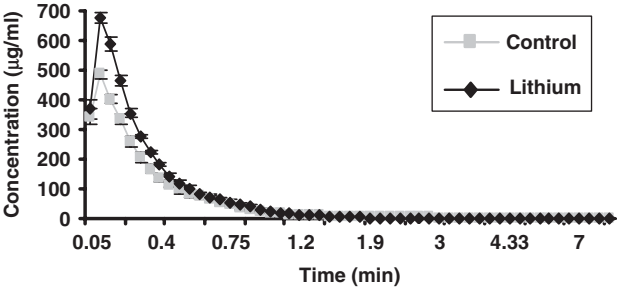

Figure 2. Concentration curves of paraquat in the efferent fluid of the isolated rat lung preparation after a bolus injection at 1000 µg for the control and LiCl groups. Mean values and SD are plotted, and are derived from 48 to 55 determinations for each preparation.

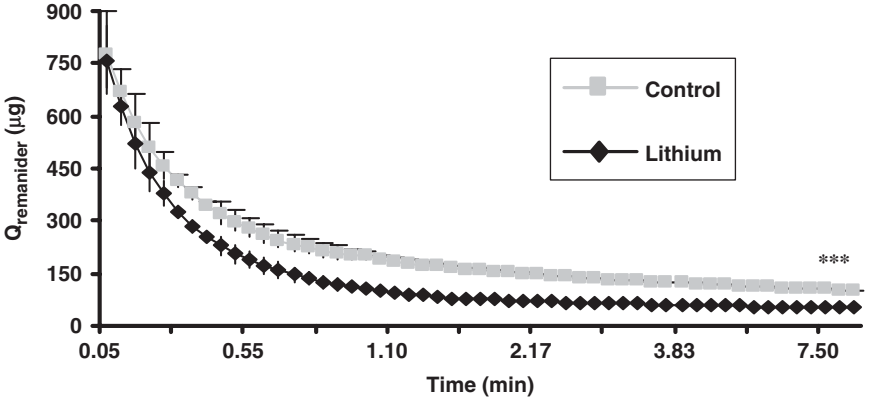

Figure 3. Paraquat concentrations remaining in the lung of control and LiCl groups after a bolus injection at 1000 µg. Mean values and SD are plotted, and are derived from 48 to 55 determinations for each preparation. ***Significant differences at $p < 0.001$ using a Student's *t*-test for non-paired samples to compare the two groups relatively to the remaining paraquat quantity after 20 min of perfusion.

obtained from the quantitation of remaining paraquat concentrations in the isolated lung at the end of the experiments (0.32 ± 0.04 and $0.18 \pm 0.02\,\mu g\,g^{-1}$ for standard and Na^+-depleted media, respectively; $p < 0.001$). The same result was obtained plotting the quantity of paraquat remaining in the lung against time (Figure 3) and shows that Na^+ depletion reduces paraquat accumulation by decreasing its access to extravascular structures of the lung tissues ($p < 0.001$). Moreover, after 30 min of perfusion, the Na^+ substitution by Li^+ also conferred a substantial protection against paraquat-induced lung oedema, as observed by the development of translucent areas (Figure 4) as well as by alterations in the hydrostatic pressure at arterial level (13 ± 2 vs. 20 ± 7 mm Hg). The differences found in the outflow curves are reflected in the parameters estimated by the statistical analysis of these curves. Table I includes the mean values of estimated parameters, by stochastic methods, corresponding to standard and Na^+-depleted media, respectively. Although all parameters are modified in the experiments with the iso-osmotic replacement of Na^+ by Li^+, only the mean values of AUC and V_d/L_w show statistically significant differences ($p < 0.01$). The mean

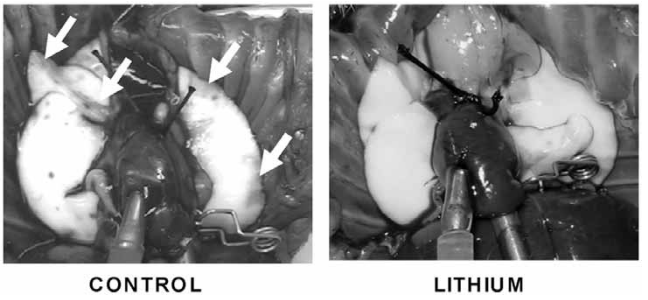

Figure 4. Macroscopic lung examination of the control and LiCl groups after a bolus injection of 1000 μg of paraquat. Photographs were taken 30 min after paraquat injection. Arrows indicate translucent areas as a result of lung oedema development.

Table I. Mean parameters estimated from outflow curves of paraquat in the isolated rat lung as evaluated by stochastic methods.

Parameter	Control group ($n = 8$), mean ± SD[8]	LiCl group ($n = 8$), mean ± SD
$AUC_{0-\infty}$ ($\mu g\,min\,ml^{-1}$)[a]	184.25 ± 15.85	219.51 ± 17.51**
MTT (min)[b]	0.74 ± 0.07	0.54 ± 0.1
VTT[c]	1.75 ± 0.52	0.64 ± 0.36
K_w (min^{-1})[d]	0.40 ± 0.06	0.63 ± 0.33
V_d (ml)[e]	3.70 ± 0.36	2.69 ± 0.52
V_d/L_w ($ml\,g^{-1}$)[f]	2.99 ± 0.38	2.21 ± 0.4**
C_{max} ($\mu g\,ml^{-1}$)[g]	491.59 ± 29.05	679.62 ± 43.04***

[a] Area under the curve.
[b] Mean transit time.
[c] Variance of mean transit time.
[d] Washout rate constant.
[e] Apparent volume of distribution.
[f] Distribution coefficient.
[g] Maximum concentration reached in the outflow samples.
Data are means ± standard deviation, derived from 48 to 55 determinations for each preparation.
Significant differences at $^{**}p < 0.01$ and $^{***}p < 0.001$, respectively, using a Student's *t*-test for non-paired samples to compare the two groups.

AUC for the efferent fluid increases, whereas the distribution coefficient in the lung (V_d/L_w) decreases, both changes revealing a lower exposure of the tissue to paraquat when the isolated lung was perfused under Na^+-depleted conditions. In fact, the mean value of MTT_a, which is the first moment of the curve that constitutes an excellent indicator of tissue exposure (Weiss and Roberts 1996), also decreases from 0.74 ± 0.07 to 0.54 ± 0.10 min, although the statistical comparison failed to show significant differences.

Discussion

Despite paraquat being the most toxic herbicide marketed over the last 60 years, it is the third most widely used product in the world for this purpose (Wesseling et al. 1997, 2001).

Nowadays, no antidote or effective treatment for paraquat poisoning has been identified, survival depending on the amount ingested and the time elapsed until beginning intensive medical measures to inactivate and eliminate paraquat. Nevertheless, attempts to elucidate the tissue-uptake mechanism to interfere with the process and to avoid the final toxicological consequences are being undertaken.

The main objective of the present study was to investigate the kinetics of paraquat in the isolated rat lung model. We have determined the kinetic parameters and the influence of Li^+ in the observed kinetics. The characterization of the kinetic profile of xenobiotics in specific organs or tissues is becoming increasingly interesting since pharmacological and toxicological responses are much more related to the concentrations at target sites than in plasma. This is even more important in the case of paraquat because the kinetics are an important issue in intoxication by this compound. The techniques of tissue isolation and perfusion offer an excellent alternative to traditional methodology when detailed information about the drug distribution in a particular body tissue is required. This technique allows the characterization of the kinetic profile for a tissue in a single animal and avoids the inter-individual variability in each single curve, leading to a corresponding reduction in curve replicates and hence a substantial reduction in the number of animals used (5–8 vs. 50–80 per tissue). The results of the comparative study on the disposition of paraquat in the presence of different media compositions in the isolated rat lung confirm these advantages and show that the data provided by this experimental model afford very useful information about the kinetic behaviour of xenobiotics in this tissue. Indeed, by using the perfused organ, compounds of interest are delivered to the structurally intact lung via the pulmonary circulation.

The paraquat outflow concentration curves (Figure 2) obtained for the control group confirms the high pulmonary affinity of this compound. The polyexponential profile shown by the curves reveals rapid access to extravascular spaces with a slow washout process. After reaching the peak value, the profile shows a three-phase decay, each phase presumably representing the washout of the product from the vascular, interstitial and intracellular spaces, respectively. Curves (Figure 2) corresponding to the experiments performed under Na^+-depleted and standard conditions show a similar profile for both efferent fluids, although the peak concentration reaches a significantly higher value in the Na^+-depleted media.

This latter observation leads to the conclusion that tissue uptake of paraquat is reduced when the iso-osmotic replacement of NaCl by LiCl is performed. Such a conclusion is also supported and confirmed by the results obtained from the quantitation of paraquat remaining in the lungs of both groups at the end of the experiments and from the premature oedema development in the control compared with the perfusion in absence of Na^+ (Figure 4). The early appearance of oedema leads to an increase in hydrostatic pressure at the arterial level reflecting a resistance to perfusion as a consequence of water accumulation in the lung. The slope of the different exponential phases can be estimated, the value for the terminal one being much lower than those corresponding to earlier phases. This may be interpreted as the existence of an inefficient export process of paraquat from the tissue. Nevertheless, an efficient lung polyamine uptake system used by paraquat to be transported into the alveolar lung epithelium seems to be operating since the product accumulates and reaches a much higher concentration in the lung than in the outflow media. Ten minutes after starting sample collection no paraquat was detected in the outflow samples in both groups. In spite of this finding, paraquat was found in lung tissue after 20 min of perfusion. Again, this may reflect the difficulty for paraquat to return to the vascular space after reaching the extravascular space (especially the alveolar epithelium). In general, a lower

tissue exposure may be due to either a more restricted access of the product to the lung or to a more rapid wash-out from the intracellular compartments. In this experiment, the significant increase of the AUC value together with the higher peak value (in the Na^+-depleted medium conditions) suggests a more restricted access of paraquat under Na^+-depleted conditions, a conclusion also supported by the significant decrease of the distribution coefficient of paraquat. The present study resulted in a peak concentration of about 500 mg l^{-1} (=1.95 mmol l^{-1}) in the effluent perfusate for the standard conditions and a value of 0.21 mmol l^{-1} for the saturable paraquat uptake transport constant (K_m) has been reported in lung slices (Ross and Krieger 1981). Accordingly, the uptake transport system was probably saturated under our experimental conditions.

Although statistical comparison failed to show significant differences in the MTT_a between the groups, the MTT_a in the lungs for the standard conditions was higher, possibly implying a longer and more intense exposure of the tissue to paraquat. These data were corroborated by the values of the distribution coefficients (V_d/L_w), which also decreased in the Li^+ medium (2.21 ml g^{-1}) in comparison with the standard conditions (2.99 ml g^{-1}).

Despite a sustained effort over the last decade, the mammalian polyamine transporter has not yet been cloned and characterized. Considering the reported mechanism of accumulation of paraquat in the lung tissue, and some reports that points to a Na^+ dependence of the polyamine uptake system (Janne et al. 1978; Rinehart and Chen 1984; Kumagai and Johnson 1988; Rannels et al. 1989; Aziz et al. 1994), it might be suggested that paraquat uptake into the extravascular compartments of the lung (alveolar interstitium and epithelium) is prevented by Na^+ depletion. In contrast, some reports evidence no Na^+ requirement for putrescine uptake by different cell types (Lewis et al. 1989; Morgan 1992).

The present study offers new data by demonstrating that the polyamine uptake system for paraquat is in fact Na^+-dependent. However, other polyamine uptake systems exist (Rannels et al. 1989) for which competition studies have shown that for their substrate uptake there is no Na^+ dependence (Smith and Wyatt 1981). It must be also considered that the lung is a heterogeneous tissue comprised of approximately 40 different cell types (Sorokin 1970). Therefore, the total tissue uptake observed in the lung reflects the mean uptake activity of all the constitutive cell types present in the tissue.

Taken collectively, it can be concluded that the kinetic behaviour of paraquat in the isolated lung seems to be modified by Na^+ depletion in the perfusion medium. Accordingly, although it seems that this condition does not significantly contribute to improve the elimination of paraquat from the tissue once the product gets to the deepest structures, we suggest that an impaired access to the lung tissue might be operating under Na^+-depletion conditions.

Acknowledgements

This work is part of a Research Project (PM 1998-0138) funded by the Spanish Council for Science and Technology. Ricardo Dinis acknowledges the FCT for his PhD grant (SFRH/BD/13707/2003).

References

Aziz SM, Lipke DW, Olson JW, Gillespie MN. 1994. Role of ATP and sodium in polyamine transport in bovine pulmonary artery smooth cells. Biochemistry and Pharmacology 48:1611–1618.

Blaszczynski M, Litwinska J, Zaborowska D, Bilinski T. 1985. The role of respiratory chain in paraquat toxicity in yeast. Acta Microbiologica Polonica 34:243–254.

Burk RF, Lawrence RA, Lane JM. 1980. Liver necrosis and lipid peroxidation in the rat as a result of paraquat and diquat administration. Effect of selenium deficiency. Journal of Clinical Investigation 65:1024–1031.

Bus JS, Aust SD, Gibson JE. 1974. Superoxide- and singlet oxygen-catalyzed lipid peroxidation as a possible mechanism for paraquat (methyl viologen) toxicity. Biochemical and Biophysical Research Communications 58:749–755.

Bus JS, Aust SD, Gibson JE. 1975. Lipid peroxidation: A possible mechanism for paraquat toxicity. Research Communications in Chemistry, Pathology and Pharmacology 11:31–38.

Clejan L, Cederbaum AI. 1989. Synergistic interaction between NADPH-cytochrome P-450 reductase, paraquat and iron in the generation of active oxygen radicals. Biochemistry and Pharmacology 38:1779–1786.

Dicker E, Cederbaum AI. 1991. NADH-dependent generation of reactive oxygen species by microsomes in the presence of iron and redox cycling agents. Biochemistry and Pharmacology 42:529–535.

Dinsdale D, Preston SG, Nemery B. 1991. Effects of injury on [3H]putrescine uptake by types I and II cells in rat lung slices. Experimental Molecular Pathology 54:218–229.

Fell AF, Jarvie DR, Stewart MJ. 1981. Analysis for paraquat by second- and fourth-derivative spectroscopy. Clinical Chemistry 27:286–292.

Fuke C, Ameno K, Ameno S, Kiriu T, Shinohara T, Sogo K, Ijiri I. 1992. A rapid, simultaneous determination of paraquat and diquat in serum and urine using second-derivative spectroscopy. Journal of Analytical Toxicology 16:214–216.

Fukushima T, Yamada K, Hojo N, Isobe A, Shiwaku K, Yamane Y. 1994. Mechanism of cytotoxicity of paraquat. III. The effects of acute paraquat exposure on the electron transport system in rat mitochondria. Experiments in Toxicology and Pathology 46:437–441.

Fukushima T, Yamada K, Isobe A, Shiwaku K, Yamane Y. 1993. Mechanism of cytotoxicity of paraquat. I. NADH oxidation and paraquat radical formation via complex I. Experiments in Toxicology and Pathology 45:345–349.

Gordonsmith RH, Brooke-Taylor S, Smith LL, Cohen GM. 1983. Structural requirements of compounds to inhibit pulmonary diamine accumulation. Biochemistry and Pharmacology 32:3701–3709.

Hirai K, Witschi H, Cote MG. 1985. Mitochondrial injury of pulmonary alveolar epithelial cells in acute paraquat intoxication. Experimental Molecular Pathology 43:242–252.

Janne J, Poso H, Raina A. 1978. Polyamines in rapid growth and cancer. Biochimica et Biophysica Acta 473:241–293.

Kumagai J, Johnson LR. 1988. Characteristics of putrescine uptake in isolated rat enterocytes. American Journal of Physiology 254:G81–G6.

Kuo TL, Lin DL, Liu RH, Moriya F, Hashimoto Y. 2001. Spectra interference between diquat and paraquat by second derivative spectrophotometry. Forensic Science International 121:134–139.

LaVoie MJ, Hastings TG. 1999. Peroxynitrite- and nitrite-induced oxidation of dopamine: Implications for nitric oxide in dopaminergic cell loss. Journal of Neurochemistry 73:2546–2554.

Lewis CP, Haschek WM, Wyatt I, Cohen GM, Smith LL. 1989. The accumulation of cystamine and its metabolism to taurine in rat lung slices. Biochemical Pharmacology 38:481–488.

Lowry OHN, Rosebrough NJ, Farr AL, Randall RJ. 1951. Protein measurement with Folin phenol reagent. Journal of Biology and Chemistry 193:265–275.

Martinez MSM, Gandarillas CIC, Lanao JM, Sanchez Navarro A. 2005. Influence of flow rate on the disposition of levofloxacin and netilmicin in the isolated rat lung. European Journal of Pharmaceutical Science 24:325–332.

Morgan DM. 1992. Uptake of polyamines by human endothelial cells. Characterization and lack of effect of agonists of endothelial function. Biochemical Journal 286:413–417.

Nemery B, Smith LL, Aldridge WN. 1987. Putrescine and 5-hydroxytryptamine accumulation in rat lung slices: Cellular localization and responses to cell-specific lung injury. Toxicology and Applied Pharmacology 91:107–120.

Onyeama HP, Oehme FW. 1984. A literature review of paraquat toxicity. Veterinary and Human Toxicology 26:494–502.

Rannels DE, Kameji R, Pegg AE, Rannels SR. 1989. Spermidine uptake by type II pneumocytes: Interactions of amine uptake pathways. American Journal of Physiology, Lung Cell and Molecular Physiology 257:L346–L353.

Rannels DE, Pegg AE, Clark RS, Addison JL. 1985. Interaction of paraquat and amine uptake by rat lungs perfused in situ. American Journal of Physiology, Endocrinology and Metabolism 249:E506–E513.

Rinehart CAJ, Chen KY. 1984. Characterization of the polyamine transport system in mouse neuroblastoma cells. Effects of sodium and system A amino acids. Journal of Biology and Chemistry 259:4750–4756.

Rose MS, Smith LL, Wyatt I. 1974. Evidence for energy-dependent accumulation of paraquat into rat lung. Nature 252:314–315.

Ross JH, Krieger RI. 1981. Structure–activity correlations of amines inhibiting active uptake of paraquat (methyl viologen) into rat lung slices. Toxicology and Applied Pharmacology 59:238–249.

Smith LL. 1982. The identification of an accumulation system for diamines and polyamines into the lung and its relevance to paraquat toxicity. Archives in Toxicology Suppl 5:1–14.

Smith LL, Wyatt I. 1981. The accumulation of putrescine into slices of rat lung and brain and its relationship to the accumulation of paraquat. Biochemistry and Pharmacology 30:1053–1058.

Sorokin SP. 1970. The cells of the lungs. In: Nettesheim P, Hanna MG, Deatheridge JW, editors. Morphology of experimental respiratory carcinogenesis. Washington, DC: US Atomic Energy Commission.

Tawara T, Fukushima T, Hojo N, Isobe A, Shiwaku K, Setogawa T, Yamane Y. 1996. Effects of paraquat on mitochondrial electron transport system and catecholamine contents in rat brain. Archives in Toxicology 70:585–589.

Thakar JH, Hassan MN. 1988. Effects of 1-methyl-4-phenyl-1,2,3,6-tetrahydropyridine (MPTP), cyperquat (MPP+) and paraquat on isolated mitochondria from rat striatum, cortex and liver. Life Sciences 43:143–149.

Tomita M. 1991. Comparison of one-electron reduction activity against the bipyridylium herbicides, paraquat and diquat, in microsomal and mitochondrial fractions of liver, lung and kidney (*in vitro*). Biochemistry and Pharmacology 42:303–309.

Weiss M. 1995. Distribution kinetics in the body and single organs: Moment analysis. In: D'Argenio DZ, editor. Advanced methods of pharmacokinetics and pharmacodynamic system analysis. New York, NY: Plenum. pp 89–100.

Weiss M, Roberts MS. 1996. Tissue distribution kinetics as determinant of transit time dispersion of drugs in organs: Application of a stochastic model to the rat hindlimb. Journal of Pharmacokinetics and Biopharmacology 24:173–196.

Wesseling C, Hogstedt C, Picado A, Johansson L. 1997. Unintentional fatal paraquat poisonings among agricultural workers in Costa Rica: Report of 15 cases. American Journal of Industrial Medicine 32:433–441.

Wesseling C, van Wendel de Joode B, Ruepert C, Leon C, Monge P, Hermosillo H, Partanen TJ. 2001. Paraquat in developing countries. International Journal of Occupational and Environmental Health 7:275–286.

Yamada K, Fukushima T. 1993. Mechanism of cytotoxicity of paraquat. II. Organ specificity of paraquat-stimulated lipid peroxidation in the inner membrane of mitochondria. Experiments in Toxicology and Pathology 45:375–380.

Yamaoka K, Nakagawa T, Uno T. 1978. Statistical moments in pharmacokinetics. Journal of Pharmacokinetics and Biopharmacology 6:547–558.

Youngman RJ, Elstner EF. 1981. Oxygen species in paraquat toxicity: The crypto-OH radical. FEBS Letters 129:265–268.